A Seminar Paper on

Antimicrobial activities of emerging nanomaterial MXenes

Course Title: Seminar

Course Code: SSC 698

Submitted to

Course Instructors

Dr. A. K. M. Aminul Islam
Professor,
Department of Genetics and Plant Breeding,
BSMRAU.

Dr. Satya Ranjan Saha
Professor,
Department of Agroforestry and Environment,
BSMRAU.

Dr. Shaikh Shamim Hasan
Professor,
Dept. of Agricultural Extension and Rural Development
BSMRAU.

Dr. Dinesh Chandra Shaha
Associate Professor,
Department of Fisheries Management,
BSMRAU.

Major Professor

Dr. Md. Tofazzal Islam
Professor and Founding Director,
Institute of Biotechnology and Genetic Engineering (IBGE),
BSMRAU, Gazipur.

Submitted by

Tasnim Zerin Khan
Reg. No.: 17-05-4214
MS Student
Term: Winter, 2022
Institute of Biotechnology and Genetic Engineering (IBGE), BSMRAU.

BANGABANDHU SHEIKH MUJIBUR RAHMAN AGRICULTURAL UNIVERSITY

GAZIPUR-1706

Abstract

MXenes are a group of two-dimensional (2D), atomically thin transition metal carbides and carbonitride with a variety of desirable properties. We looked at the antibacterial capabilities of Ti3C2Tx MXene to better understand the effects of the novel 2D carbides on microbes . Gram-positive and gram-negative microorganisms were used to assess Ti3C2Tx's antibacterial abilities. When compared to graphene oxide (GO), which has been frequently reported as an antibacterial agent, Ti3C2Tx exhibits a higher antibacterial effectiveness. This review examines concentration- and size-dependent antibacterial activity. MXenes having considerable anti-fouling and bactericidal capabilities were further validated after exploring the antibacterial mechanism analysis in different ongoing research experiments.

Key words: MXenes, Antibiotic resistance, nanomaterials, Antimicrobial Activity.

TABLE OF CONTENT

SL. NO.	NAME OF THE TOPIC		PAGE NO.
1.	ABSTRACT		**ii**
2.	TABLE OF CONTENTS		**iii**
3.	LIST OF TABLES		**iv**
4.	LIST OF FIGURES		**iv**
5.	Chapter I	INTRODUCTION	**1-2**
6.	Chapter II	MATERIALS AND METHODS	**3**
7.	Chapter III	REVIEW OF FINDINGS	**4-20**
		3.1 Origin and Discovery of MXenes	**4**
		3.2 Synthesis process of MXenes	**6**
		3.3 Antibacterial Activity of MXene	**8**
		3.3.1 Delamination- dependent antibacterial activity	**9**
		3.3.2 Concentration- dependent antibacterial activity	**11**
		3.3.2a Concentration- dependent cell viability measurement compared to GO	**12**
		3.3.2b Concentration- dependent cell viability measurement between gram (+) and gram (-) bacteria	**12**
		3.3.3 Size- dependent antibacterial activity	**14**
		3.3.4 Cytotoxicity measured by LDH release assay	**15**
		3.4 Proposed Antibacterial Mode of Action of MXene nanosheets	**17**
		3.5 Prospects of MXenes	**20**
8.	Chapter IV	CONCLUSION	**21**
9.	REFERENCES		**22**

LIST OF TABLES

TABLE NO.	TITLE	PAGE
Table 1.	Specific growth constant and doubling time obtained in the batch growth tests for *E. coli* and *B. subtilis* cells treated to different $Ti_3C_2T_x$ concentrations.	**14**

LIST OF FIGURES

FIGURE NO.	TITLE	PAGE
Figure 1.	Periodic tables showing compositions of MXenes and MAX phases.	**4**
Figure 2.	Timeline of MXene: a journey from 2011 to now.	**5**
Figure 3.	(a) Structure of layered Ti_3AlC_2. (b) Terminated MXene. (c) Schematic showing preparation of MXene from MAX phases.	**7**
Figure 4.	Schematic of the exfoliation process for Ti_3AlC_2	**7**
Figure 5.	SEM images of Ti_3AlC_2 (A) and ML-$Ti_3C_2T_x$ (B) and $Ti_3C_2T_x$ nanosheets on an alumina filter (C).	**9**
Figure 6.	(A) Photographs of agar plates onto which E. coli (top panel) and B. subtilis (bottom panel) bacterial cells were re-cultivated after treatment for 4 h with a control (a), and 100 µg/mL of Ti_3AlC_2 (b), ML-Ti_3C_2Tx (c), and delaminated Ti_3C_2Tx (d). (B) Percentage growth inhibition of bacterial cells treated with 100 µg/mL of	**10**

	Ti_3AlC_2, ML-$Ti_3C_2T_x$, and delaminated $Ti_3C_2T_x$.	
Figure 7.	Concentration-dependent antibacterial activities of the $Ti_3C_2T_x$ in aqueous suspensions	**11**
Figure 8.	Cell viability measurements of (A) E. coli and (B) B. subtilis treated with Ti_3C_2Tx and graphene oxide (GO) in aqueous suspension.	**12**
Figure 9.	Antibacterial activity of 100 µg/mL MXene nanosheets of 0.09- and 0.57µg/ml sizes against B. subtilis and E. coli was investigated by fluorescence imaging.	**15**
Figure 10.	Ti_3C_2Tx cytotoxicity measured by LDH release from the bacterial cells exposed to different concentrations of Ti_3C_2Tx for 4 h.	**16**
Figure 11.	Schematic representation of proposed antibacterial MoA of MXene nanosheets.	**17**
Figure 12.	SEM images of the E. coli (top panel) and B. subtilis (bottom panel) treated with 0 µg/mL – control (A), 50 µg/mL (B), and 100 µg/mL of Ti_3C_2Tx, at low and high magnification, respectively.	**18**
Figure 13.	TEM images of E. coli (A, B) and B. subtilis (C, D) treated with 200 µg/mL of Ti_3C_2Tx for 4 h at low (A, C) and high magnifications (B, D).	**19**

CHAPTER I
INTRODUCTION

Antimicrobial resistance is a significant issue in agriculture since it has an impact on the security of the food supply as well as the health of both humans and animals. According to reports, China consumes around half of all antibiotics used in animal husbandry worldwide, followed by the US, Brazil, India, and Germany (Laxminarayan & Boeckel, 2015). When we examine the global consumption of different antibiotics, we can see that the greatest user of antimicrobials for livestock in 2010 was reported to be China, which used up to 30% of the world's total antimicrobial output. At the present rate of usage, India is the next largest consumer of antimicrobials for the care and production of livestock, trailing China, and the top three users of antibiotics in developed nations in 2015 were the United States, France, and Italy, while India, China, and Pakistan topped the list in developing nations (Klein *et al*., 2018). In 2015, the United States, France, and Italy were the top three users of antibiotics, while India, China, and Pakistan led the list of emerging nations, with a 65% rise in consumption recorded globally between 2000 and 2015 (Ganguly *et al.*, 2011). A research predicted that by 2030, the use of antibiotics will increase by 67% in a number of the world's most populous nations, including India (Boeckel *et al.*, 2015). The present century has seen a significant increase in the emergence of microbes due to this overuse of antibiotics, and these microbes have been observed to modify their genes more quickly and effectively, aiding them in developing resistance against various antibiotic groups, particularly broad-spectrum antibiotics. Researchers are reporting that even the latest iteration of antibiotics are ineffective against these microbes, making this a challenging problem to address. If the current situation holds, we may transition into a post-antibiotic period in which medications may not be able to treat even the most basic infections.

In order to prevent infections from developing resistance and to offer secure, productive methods for managing illness and safeguarding crop yields, new antimicrobial materials are required for agriculture. For instance, using nanoparticles to manage plant infections and pests while utilizing less pesticides has shown promise. The term "nanomaterials" refers to a class of substances that, usually, have dimensions smaller than 100 nanometers and display distinctive characteristics at the

nanoscale (nm). At this size, quantum mechanics controls how matter behaves, giving rise to a variety of unique chemical and physical characteristics. The growth of nanotechnology in recent years has created new opportunities for the creation of sophisticated materials with distinctive features and uses. In conventional pesticides, only about 0.1% are uptaken by target species while the rest 99.9% lost due to spray drift and dust drift, leaching and by rolling down into different environmental media (Pimentel & Burgess, 2012). Whereases, use of nanomaterials aids in lowering the quantity of antimicrobials used in agriculture, and the pathogens are better controlled while having a less negative environmental effect because of nanomaterials' ability to deliver targeted and sustained release of active chemicals. Analysis demonstrates that the total performance of nano pesticides against target species is 31.5% greater when compared to non-nanoscale pesticides, including an 18.9% increase in efficacy in field experiments. The toxicity of nanopesticides for non-target species is noticeably 43.1% lower, demonstrating a reduction in environmental collateral harm (Wang et al., 2022). A new family of compounds called MXenes has recently attracted interest due to its antibacterial capabilities. MXenes, which are two-dimensional (2D) transition metal carbides or nitrides with large surface area and distinctive electrical characteristics, are excellent prospects for a variety of uses, including energy storage, water purification, and biomedicine. In this regard, the capacity of MXenes to suppress the development of bacteria, viruses, and fungus opens up a promising new route for the creation of novel antimicrobial drugs.

The objectives of this paper are:

1. To review the emerging research on the antimicrobial activities of MXenes including their mechanisms of action.
2. To explore their potential as biocide in order to fully utilize this cutting-edge technology.

CHAPTER II
MATERIALS AND METHODS

This paper is absolutely a review paper. So, all the information for this paper was collected from secondary sources with the intention of preparing it. The title was selected with the consultation of my major professor. I used various relevant articles and journals relevant to this topic for collecting recent information. Good suggestions, valuable information, and kind consideration from my honorable major professor and other teachers in the Institute of Biotechnology and Genetic Engineering (IBGE), Bangabandhu Sheikh Mujibur Rahman Agricultural University helped to enrich this paper. After collecting the necessary information, it has been compiled and arranged chronologically for better understanding and clarification.

CHAPTER III

REVIEW OF FINDINGS

3.1 Origin and Discovery of MXenes

MXenes are a novel class of 2D materials that were uncovered in 2011 by researchers at Drexel University (Naguib *et al*., 2011). $M_{n+1}X_n$, where M stands for transition metals (such as Sc, Ti, Zr, Hf, V, Nb, Ta, Cr, Mo, etc.), and X is either carbon or nitrogen, is the standard formula for the MXene family. The MXene family is made up of transition metal carbides, carbonitrides, and nitrides(Naguib *et al.*, 2011; Naguib & Gogotsi, 2015).

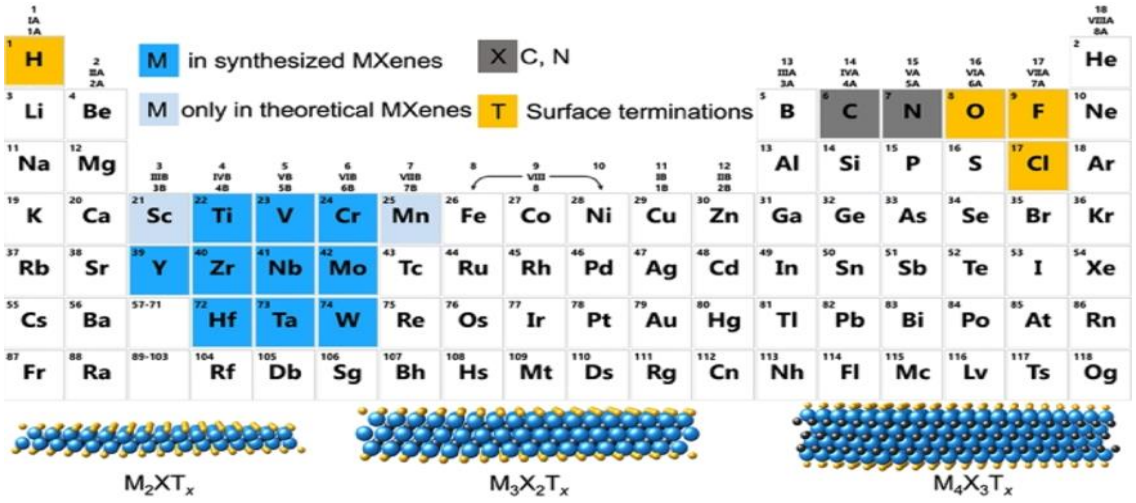

Source: (Gogotsi & Anasori, 2019)

Figure1. Periodic tables showing compositions of MXenes and MAX phases. Elements used to build MXenes. The bright blue elements represent MXenes that have not been yet experimentally confirmed. The schematics of three typical structures of MXenes are presented at the bottom.

The term "MXene" was chosen to recognize the parent ternary carbide and nitrides, or MAX phases, from which MXenes are produced as well as to emphasize the similarities between this 2D material family and graphene (Barsoum, 2013). By selectively etching Al from Ti3AlC2 with HF acid, the first MXene multilayered powder (Ti3C2Tx) was developed in 2011 (Naguib *et al*., 2011). MXenes, including Ti_2CT_x, $(Ti,Nb)_2CT_x$, $(V,Cr)_3C_2T_x$, Ti_3CNT_x, and $Ta_4C_3T_x$, were created in 2012, establishing them as a family of transition metal carbides and carbonitrides (Halim *et al.*, 2014). Single layers of MXenes were obtained in 2013 using intercalation and delamination with

organic compounds (Naguib *et al*., 2012). In 2014, HF etchants such as NH_4HF_2 (Ghidiu & Naguib, et al., 2014) or LiF/HCl (Ghidiu & Lukatskaya, *et al*., 2014) combinations were utilized in situ. The latter produced $Ti_3C_2T_x$ with clay-like characteristics and is referred to as the clay method. By sonicating $Ti_3C_2T_x$ clay in water, single flakes of $Ti_3C_2T_x$ of submicron lateral size were separated (Ghidiu & Lukatskaya, *et al.*, 2014). Large scale (high yield) delamination of various MXenes utilizing amine-assisted or TBAOH was reported in 2015 (Mashtalir *et al*., 2013, 2015). Moreover, two sub-families of MXenes, ordered-double-transition metal carbides (such as $Mo_2TiC_2T_x$, $Cr_2TiC_2T_x$, $Mo_2Ti_2C_3T_x$), with two distinct transition metals occupying separate atomic layers, were found, adding more than 25 potential possible MXenes to the family (Naguib *et al.*, 2015).With optimization of the LiF/HCl etching process, large single flakes of $Ti_3C_2T_x$ (> 2m) were delaminated and isolated without sonication in 2016. MILD is the optimized approach that allows for single-flake characterization (Anasori *et al.*, 2015). MXene with ordered divacancies ($Mo_{1.3}CT_x$) was synthesized in 2017 by synthesizing in-plane double transition metal MAX phase (($Mo_{1.3}$ Sc)AlC) and etching one of the transition metals (Tao *et al*., 2017). $Ti_3C_2T_x$ flakes on an alumina membrane are seen in SEM photos between 2014 and 2016 where the scale bars were 2 µm.

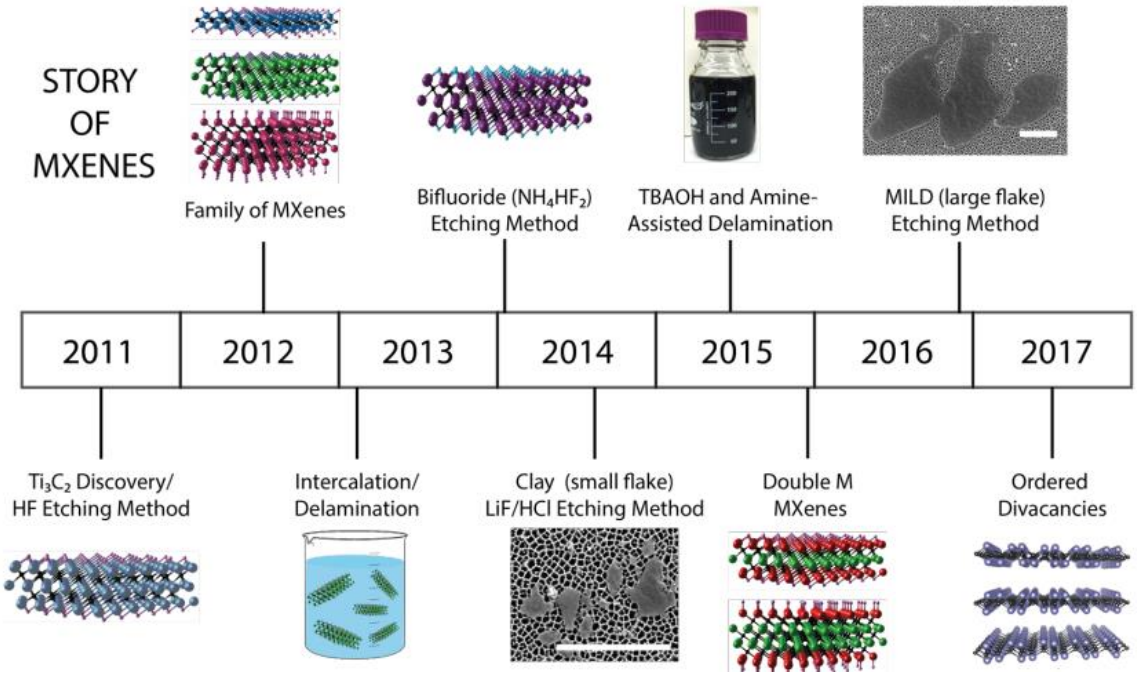

Source: (Alhabeb *et al*., 2017)

Figure2. Timeline of MXene: a journey from 2011 to now.

3.2 Synthesis process of MXenes

By carefully removing layers of *sp* components from the appropriate three-dimensional (3D) MAX phases, MXenes are created [Fig. 2(a)]. These layered ternary metal carbides, nitrides, or carbonitrides are referred to as MAX phases. They have the general formula $M_{n+1}AX_n$ (n = 1, 2, or 3), where M, A, and X stand for early d-block transition metals, main-group *sp* elements (mostly IIIA or IVA), and either or both Carbon and Nitrogen atoms, respectively. Around 70 MAX phases have been documented so far (Barsoum, 2013), however Only Ti_3C_2, Ti_2C, $(Ti_{0.5}, Nb_{0.5})_2C$, $(V_{0.5}, Cr_{0.5})_3C_2$, Ti_3CN, Ta_4C_3 (Naguib *et al.*, 2012), Nb_2C, V_2C (Naguib *et al*., 2013), and Nb_4C_3(Ghidiu, Naguib, *et al*., 2014) are members of the recognized MXene family. Importantly, during the etching process, the outer surfaces of the exfoliated layers are usually terminated with F, OH, and/or O groups [Fig. 2(b)]. These terminated MXene species are referred to as $M_{n+1}X_nT_x$, where x is the number of terminations and T is the number of surface groups (F, OH, or O). In the ground-breaking work (Naguib *et al.*, 2011), the weakly bound Al layers from the Ti_3AlC_2 phase were extracted to produce $Ti_3C_2T_x$ (T = OH and F). The HF solutions' reactions with Ti_3AlC_2 include the following:

$$Ti_3AlC_2 + 3HF = AlF_3 + 3/2H_2 + Ti_3C_2 \ldots. (1)$$

$$Ti_3C_2 + 2H_2O = Ti_3C_2 (OH)_2 + H_2 \ldots.. (2)$$

$$Ti_3C_2 + 2HF = Ti_3C_2F_2 + H_2 \ldots. (3)$$

OH and F terminations are produced by reactions (2) and (3), respectively. The solids were then separated using centrifugation, and then they were cleaned with deionized water. MXenes have multilayered structures without delamination. Sonication was used to produce single- or few-layer MXenes, but it was subsequently shown that intercalation of dimethyl sulfoxide (DMSO) was more effective (Mashtalir *et al*., 2013).

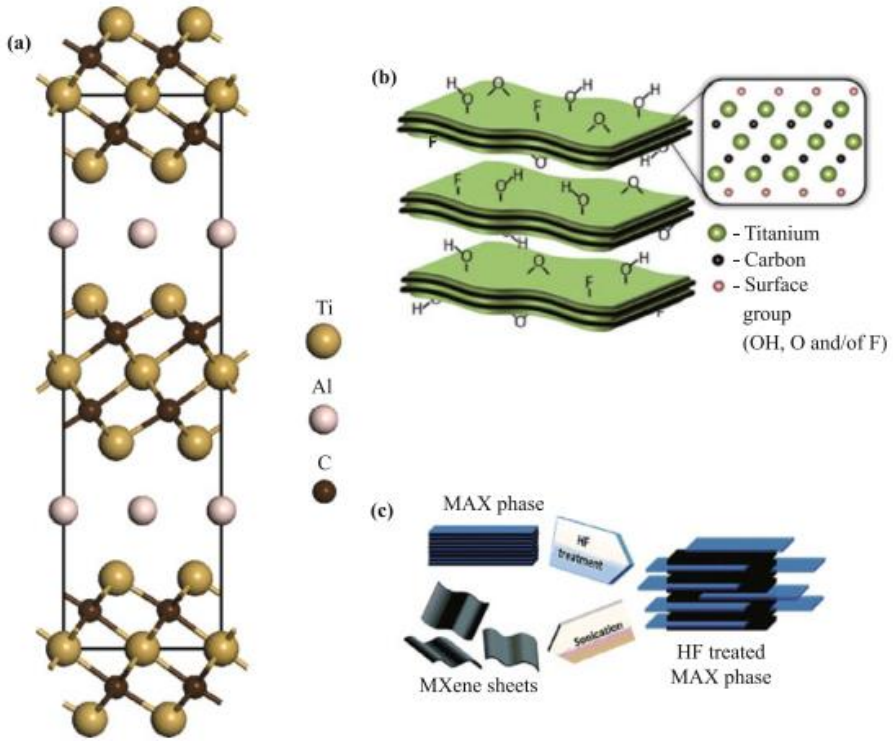

Source:(Lei et al., 2015)

Figure3. (a) Structure of layered Ti_3AlC_2. (b) Terminated MXene. Reprinted with permission from (Mashtalir *et al*., 2014) Copyright 2014 Royal Society of Chemistry. (c) Schematic showing preparation of MXene from MAX phases. Reproduced with permission from Ref. [13]. Copyright c 2012 American Chemical Society.

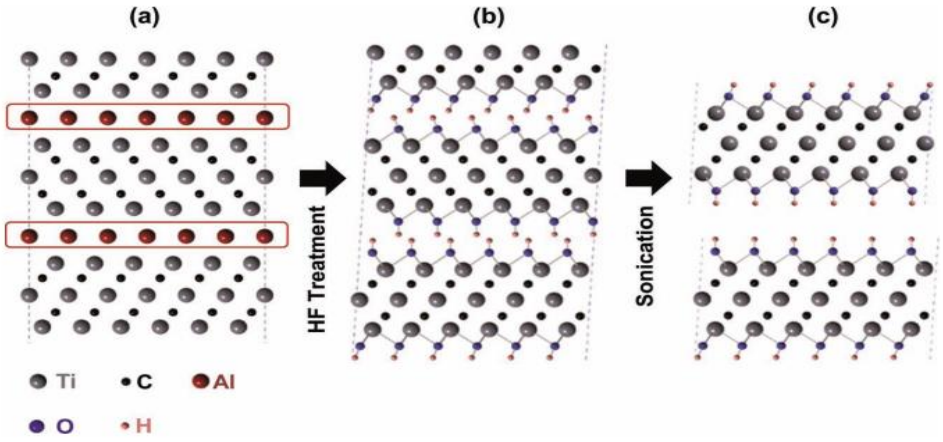

Source: (Naguib *et al*., 2011)

Figure4. Schematic of the exfoliation process for Ti_3AlC_2. a) Ti_3AlC_2 structure. b) Al atoms replaced by OH after reaction with HF. c) Breakage of the hydrogen bonds and separation of nanosheets after sonication in methanol.

3.3 Antibacterial Activity of MXene

2D graphene-based materials (graphite oxide, GO, and reduced GO (rGO)) have been studied for their antibacterial efficacy against Gram-negative and Gram-positive bacteria when they come into direct contact (Akhavan & Ghaderi, 2010; Hu *et al*., 2010; Kim *et al.*, 2014; J. Li *et al.*, 2014; Liu *et al.*, 2011; Salas *et al*., 2010; Tu *et al*., 2013). Graphene's antibacterial properties are due to both chemical and physical factors. Research has linked these properties to physical and oxidative stress caused by the sharp edges of graphene nanosheets, which can damage cell membranes and lead to their loss of integrity(Liu *et al.*, 2011; Wang *et al.*, 2014; Wu *et al.*, 2015). Apart from that, research has established the antibacterial activity of metal and metal oxide nanoparticles, such as Ag, ZnO, and TiO2 (Chernousova & Epple, 2013; Lemire *et al.*, 2013), and these nanoparticles have been linked to the formation of reactive oxygen species (ROS), direct contact with bacterial membranes, penetration of the bacteria, and interactions with DNA and proteins containing phosphorus and sulfur ultimately causing bacterial cell death (Choi & Hu, 2008; Lakshmi Prasanna & Vijayaraghavan, 2015; Y. Li *et al*., 2012; Wang *et al*., 2014; Zhang *et al.*, 2013). Furthermore, the antibacterial qualities of carbon nanotubes (CNT) based composite films have been explained by a number of processes, including the blockage of electron transports, leakage and penetration of cell membranes, and the production of ROS (Q. Li *et al*., 2008; Narayan *et al.*, 2005; Pulskamp *et al.*, 2007). So, "MXenes", a class of 2D materials having early transition metal, and carbon/ nitrogen along with graphene-like structure surely have some antibacterial activity. Despite the fact that MXenes' antibacterial capabilities have never been studied, it is logical to presume that at least some of those processes may be applicable to MXenes. MXenes already have the potential of outperforming graphene oxide (GO) membranes in the separation of higher charge cations. MXenes' antimicrobial properties, however, have never been investigated. It is crucial to research MXenes' antibacterial abilities in order to determine whether they might be used as a biocide in water treatment and biomedical applications.

Here, we give a comprehensive overview of $Ti_3C_2T_x$ MXene's antibacterial properties. The antibacterial activity of $Ti_3C_2T_x$ MXene were explored in order to better understand the health and environmental effects of the new 2D carbides. Some common bacterial models, including gram-positive *Staphylococcus aureus* (*S. aureus*), *Bacillus subtilis (B. subtilis)*, and gram-negative *Escherichia coli (E. coli*) were used and the antimicrobial properties were compared with

a standard material like 2D graphene oxide (GO). Cell viability tests, scanning electron microscopy (SEM), transmission electron microscopy (TEM), and a lactate dehydrogenase (LDH) release assay results were investigated to finally present MXenes as a novel class of 2D antibacterial nanomaterials to offer up opportunities for MXenes in the antibacterial and water purification sectors.

3.3.1 Delamination- dependent antibacterial activity

The inhibitory activity of three materials (Ti_3AlC_2 (MAX), ML-MXene, and delaminated $Ti_3C_2T_x$ nanosheets) was evaluated against both E. coli and B. subtilis in order to explore the impact of delamination on the antibacterial efficacy of MXene. The bacterial growth inhibition was measured by the colony counting method. Photographs of agar plates on which control and bacterial cells were re-cultivated after being treated for 4 hours with the same quantity of 100 µg/mL of nanomaterial are shown in Figure 6A. Figure 6B, which depicts the percentage growth inhibition of the two bacterial strains exposed to the materials, reveals that the percentage growth inhibition for E. coli and B. subtilis caused by MAX dispersion was only 14.39±1.43% and 18.34±1.59% respectively. As compared to MAX, the ML- Ti3C2Tx dispersion had somewhat more antibacterial action, inhibiting the development of E. coli and B. subtilis by 30.55±2.56% and 33.60±2.89%, respectively.

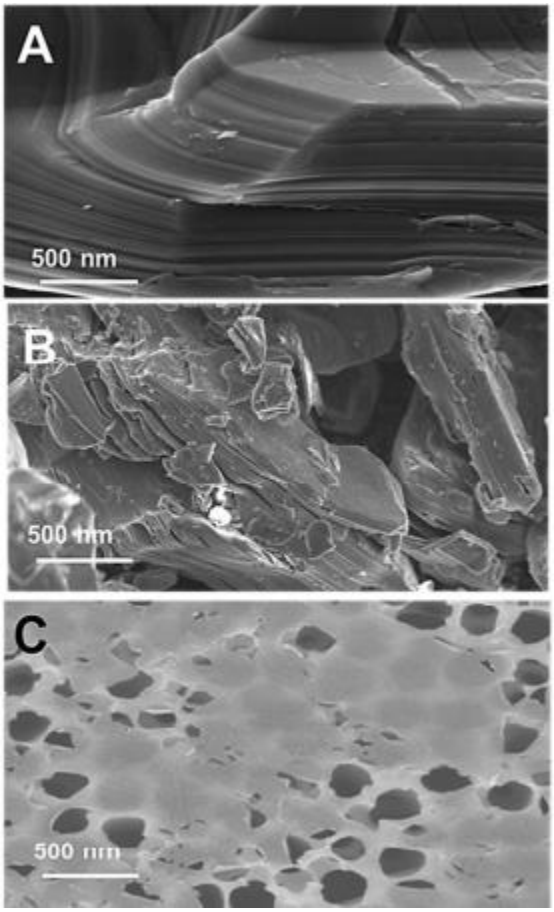

Source: (Rasool et al., 2016)

Figure 5. SEM images of Ti_3AlC_2 (A) and ML-Ti_3C_2Tx (B) and Ti_3C_2Tx nanosheets on an alumina filter (C).

The viability loss of E. coli and B. subtilis cells increases to 97.70±2.87% and 97.04±2.91% respectively, for the cells exposed to the colloidal solution of delaminated Ti3C2Tx MXene, demonstrating a significantly stronger inhibition.

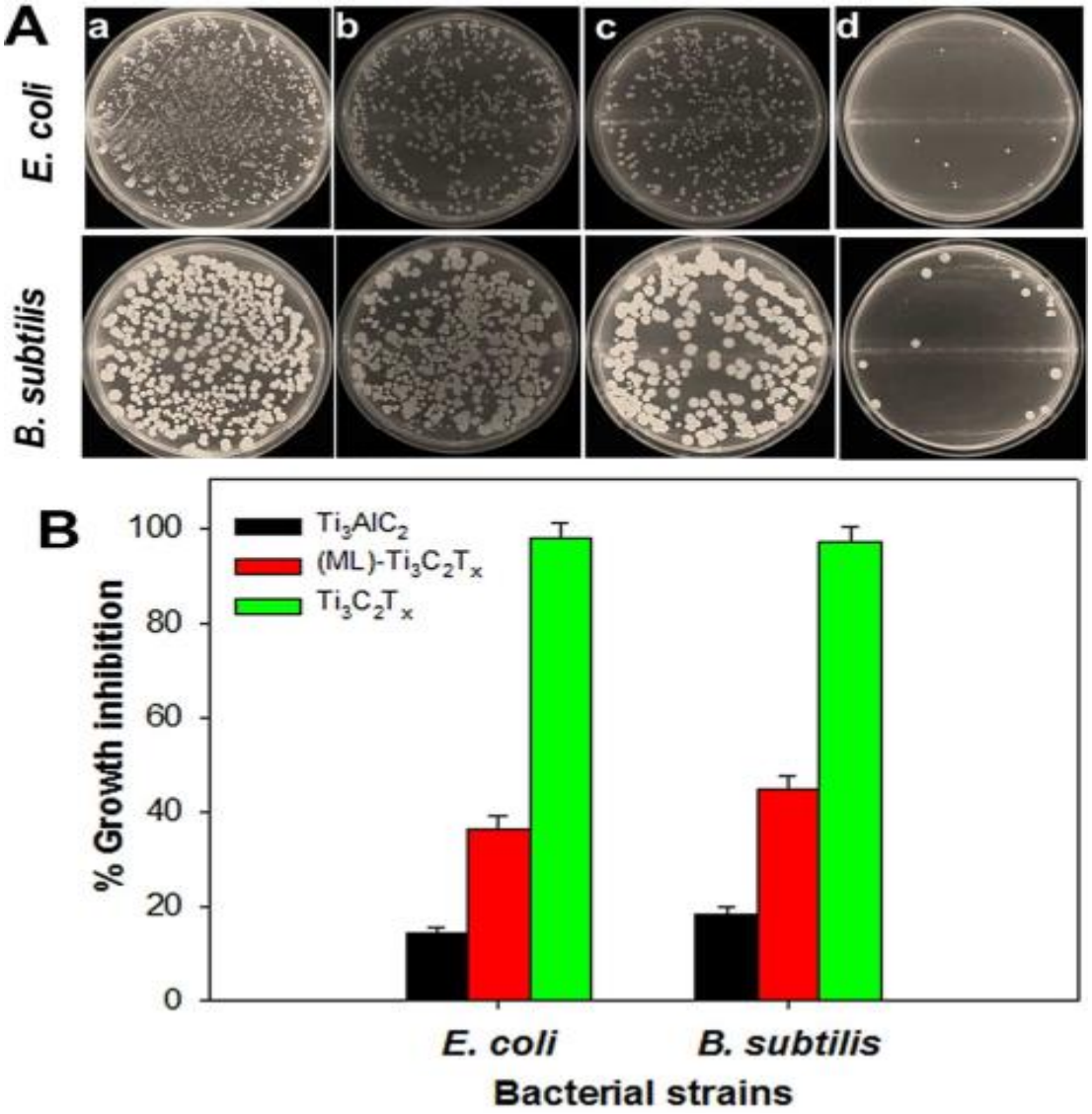

Source: (Rasool *et al.*, 2016)

Figure 6. (A) Photographs of agar plates onto which E. coli (top panel) and B. subtilis (bottom panel) bacterial cells were re-cultivated after treatment for 4 h with a control (a), and 100 µg/mL of Ti_3AlC_2 (b), ML-Ti_3C_2Tx (c), and delaminated Ti_3C_2Tx (d). (B) Percentage growth inhibition of bacterial cells treated with 100 µg/mL of Ti3AlC2, ML-Ti_3C_2Tx, and delaminated Ti_3C_2Tx. Error bars represent the standard deviation of triplicate experiments.

3.3.2 Concentration- dependent antibacterial activity

The growth curve and cell viability of Gram (+) B. subtilis and Gram (-) E. coli were measured after exposure to increasing concentrations of $Ti_3C_2T_x$ colloidal solutions. The optical density (OD) for both untreated and treated bacteria was measured spectrophotometrically at 600 nm during a range of time periods, from the lag phase to the stationary phase. After being exposed to various doses of $Ti_3C_2T_x$ for 4 hours, bacteria (at 10^7 colony forming units (CFU)/mL) were re-cultivated on agar plates and analyzed using the bacteria counting method. Figure 2 displays typical images of *E. coli* or *B. subtilis* bacteria colonies following exposure to various concentrations. Both panels show that when the concentration of $Ti_3C_2T_x$ rises, the number of colonies drastically declines. The findings show that $Ti_3C_2T_x$ has an antibacterial action that is dose-dependent. According to Pandey *et al.*, 2020 , the same result were found when using different concentration of $Nb_4C_3T_x$ sheets on against *E. coli* and *S. aureus*.

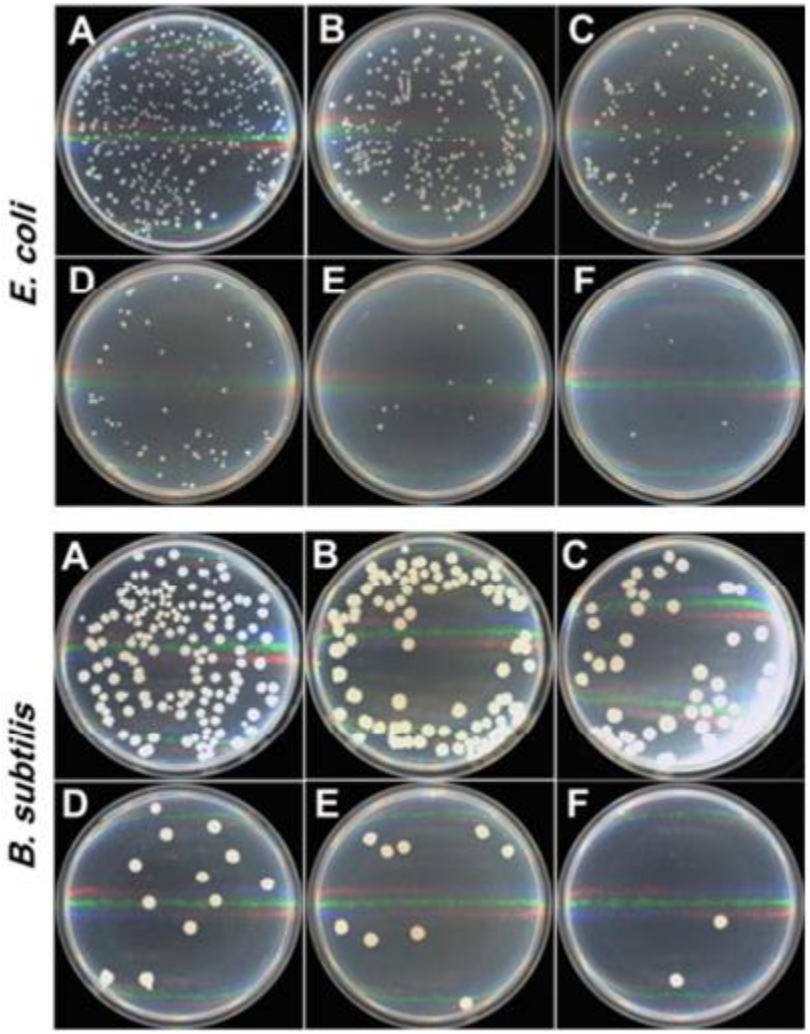

Source: (Rasool *et al.*, 2016)

Figure 7. Concentration dependent antibacterial activities of the Ti3C2Tx in aqueous suspensions: Photographs of agar plates onto which E. coli (top panel) and B. subtilis (bottom panel) bacterial cells were re-cultivated after treatment for 4 h with 0 µg/mL (A), 10 µg/mL (B), 20 µg/mL (C), 50 µg/mL (D), 100 µg/mL (E), and 200 µg/mL (D) of Ti_3C_2Tx, respectively. Bacterial suspensions in deionized water without Ti3C2Tx MXene material was used as control.

3.3.2a Concentration- dependent cell viability measurement compared to GO

In an experiment done by Rasool *et al*., 2016, bacterial suspensions (10^7 CFU/mL) were shaken at 150 rpm for 4 hours at 35 °C while being incubated with various doses of $Ti_3C_2T_x$ and GO. The colony forming count method was used to determine survival rates. Figure 8 illustrates the viability of both *E. coli* and *B. subtilis* bacteria; in the control, which was taken as 100%, and subjected to 0-200 µg/mL of GO in order to compare the antibacterial activity of $Ti_3C_2T_x$ with GO. The $Ti_3C_2T_x$ MXene has a stronger antibacterial action in that experimental setting compared to GO, as shown by the significant differences in bacterium colonies on agar plates for both bacterial strains. With 200 µg/mL of $Ti_3C_2T_x$, $Ti_3C_2T_x$ demonstrated greater than 98% cell inactivation in both bacterial strains, whereas GO produces roughly 90% inactivation at the same dose.

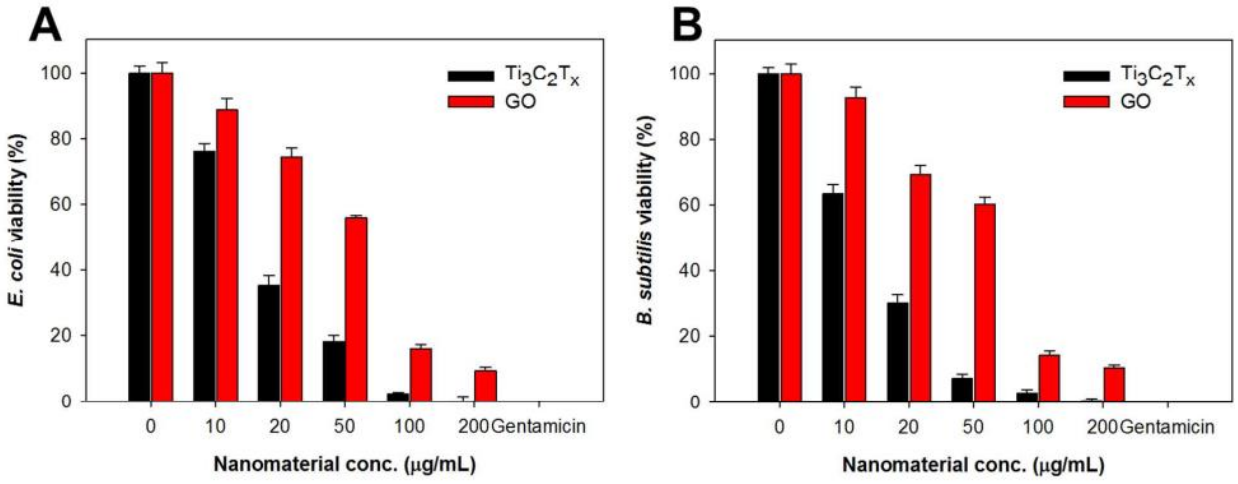

Source:(Rasool *et al*., 2016)

Figure 8. Cell viability measurements of (A) E. coli and (B) B. subtilis treated with Ti_3C_2Tx and graphene oxide (GO) in aqueous suspension.

3.3.2b Concentration- dependent cell viability measurement between gram (+) and gram (-) bacteria

In figure 8, $Ti_3C_2T_x$ demonstrated remarkable antibacterial activity when exposed to Gram (+) and Gram (-) bacteria. The lowest $Ti_3C_2T_x$ concentration of 2 µg/mL showed a 92.53% and 93.96% survival rate for *E. coli* and *B. subtilis*, respectively. The survival rates of *E. coli* and *B. subtilis* were reduced to 35.31% and 28.21% by increasing the concentration of $Ti_3C_2T_x$ MXene from 2

μg/mL to 20 μg/mL. At 100 μg/mL of $Ti_3C_2T_x$, bacterial viability loss of more than 96% was seen, and bacterial inhibition increased to more than 99% at 200 μg/mL.

The $Ti_3C_2T_x$ dispersions showed a stronger influence on B. subtilis than E. coli at lower concentrations, which is in agreement with previously reported data where different nanomaterials demonstrated greater antibacterial activity against Gram (+) bacterial strains than against Gram (-) bacteria and where differences in the cell wall structure of two bacterial strains were suggested as potential causes of different sensitivities (Fu *et al*., 2015; Hu *et al.*, 2010). *E. coli* as a Gram (-) bacteria and has an exterior protective lipid membrane despite having a significantly thinner peptidoglycan layer (thickness of 7-8 nm). Gram (+) *B. subtilis*, on the other hand, has thicker peptidoglycan cell walls that range in thickness from 20 to 80 nm but lacks the exterior lipid membrane. In comparison to Gram (-) *E. coli* with the outer membrane, it was observed that Gram (+) bacteria missing the outer membrane were more susceptible to injury from direct contact. Moreover, the isoelectric point (pI) of Gram (-) *E. coli* cells is 4-5, while Gram (+) *B. subtilis* cells have a higher pI value reaching 7, resulting in a more negatively charged surface in culture media (Guo *et al*., 2001). *E. coli* cells at pH 7 may have stronger negative charges, which may account for their greater resistance to $Ti_3C_2T_x$ substrate exposure than *B. subtilis* cells in aqueous suspensions at pH 7. This could also be explained by the reported variation in antibacterial activity between Gram (+) *B. subtilis* and Gram (-) *E. coli*. In another assay, bacterial suspensions were subjected to various $Ti_3C_2T_x$ concentrations for 4 hours at 35°C, and the reaction mixture was then transferred to 15-mL tubes with 10 mL LB medium in each. For both bacterial strains, growth kinetics constants were calculated and are shown in Table 1.

Table 1: Specific growth constant and doubling time obtained in the batch growth tests for *E. coli* and *B. subtilis* cells treated to different $Ti_3C_2T_x$ concentrations

Substrate	Constant	$Ti_3C_2T_x$ (µg/mL)						
		0	2	10	20	50	100	200
E. coli	μ_e (h^{-1})	0.277	0.271	0.261	0.239	0.168	0.087	0.068
	T_d (h)	2.5	2.550	2.65	2.9	4.12	7.92	10.11
B. subtilis	μ_b (h^{-1})	0.347	0.319	0.306	0.264	0.240	0.190	0.134
	T_d (h)	2.0	2.251	2.259	2.617	2.878	3.629	5.16

Source: (Rasool *et al.*, 2016)

It was discovered that when $Ti_3C_2T_x$ concentration increased from 0 to 200 µg/mL., the specific growth constants for *E. coli*, μ_e fell from 0.277 h^{-1} to 0.068 h^{-1}. With increasing $Ti_3C_2T_x$ concentration, *B. subtilis* growth rate constants μ_b decreased from 0.347 h^{-1} to 0.134 h^{-1}. Bacterial doubling times (T^d) for *E. coli* and *B. subtilis* rose from 2.5 h to 10.11 h and 2.0 h to 5.16 h, respectively, with a rise in $Ti_3C_2T_x$ concentration from 0 to 200 µg/mL., indicating a substantial bactericidal impact.

3.3.3 Size- dependent antibacterial activity

In another experiment done by Shamsabadi *et al.*, 2018, 100 µg/mL $Ti_3C_2T_x$ MXene nanosheets of 0.09 µm and 0.57 µm sizes against *B. subtilis* and *E. coli* investigated by fluorescence imaging. The bacteria were treated for 3 or 8 hours in the dark and bacterial population dispersion were evaluated.

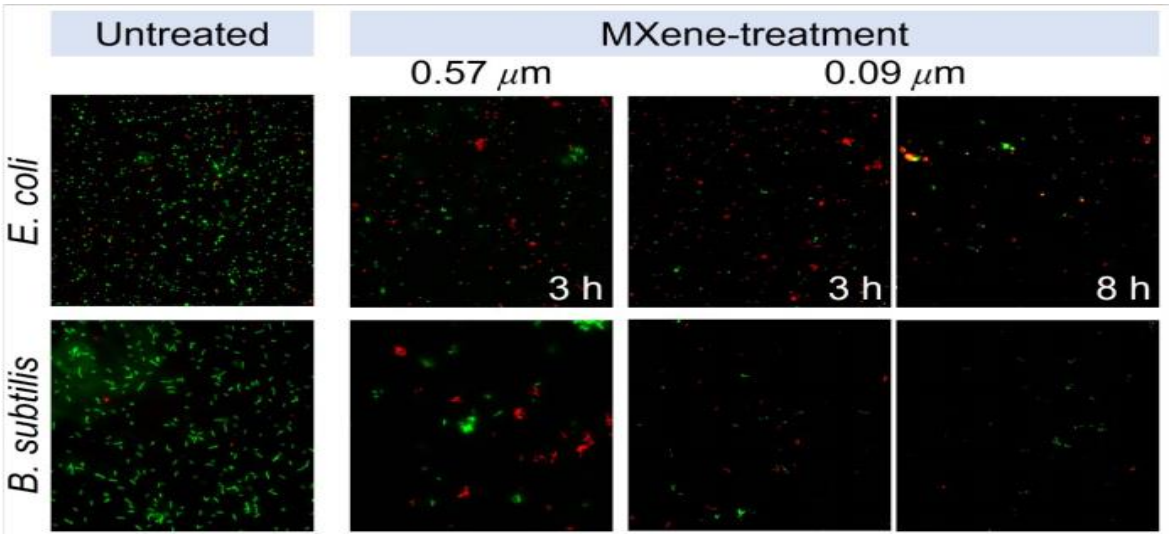

Source: (Shamsabadi *et al.*, 2018)

Figure 9. Antibacterial activity of 100 μg/ml MXene nanosheets of 0.09- and 0.57-μm sizes against *B. subtilis* and *E. coli* investigated by fluorescence imaging.

In untreated samples, there were 2-5% dead bacteria (i.e., bacteria stained with PI). Nevertheless, both bacteria samples showed a significant increase in the dead population after being exposed to 0.57- μm MXene for 3 hours. Moreover, treatment of the bacteria with the lowest lateral size nanosheets (0.09- μm MXene) led to greater populations of dead bacteria as well as lower fluorescence intensities, confirming the idea that the smaller nanosheets led to the release of DNA from the bacterial cytoplasm.

3.3.4 Cytotoxicity measured by LDH release assay

The LDH release assay was used to quantify the degree of cell injury. After 4 hours of incubation, the LDH activity in the supernatants was depicted in Figure 10. When bacteria were exposed to $Ti_3C_2T_x$ nanosheet dispersions, concentration-dependent LDH release was seen

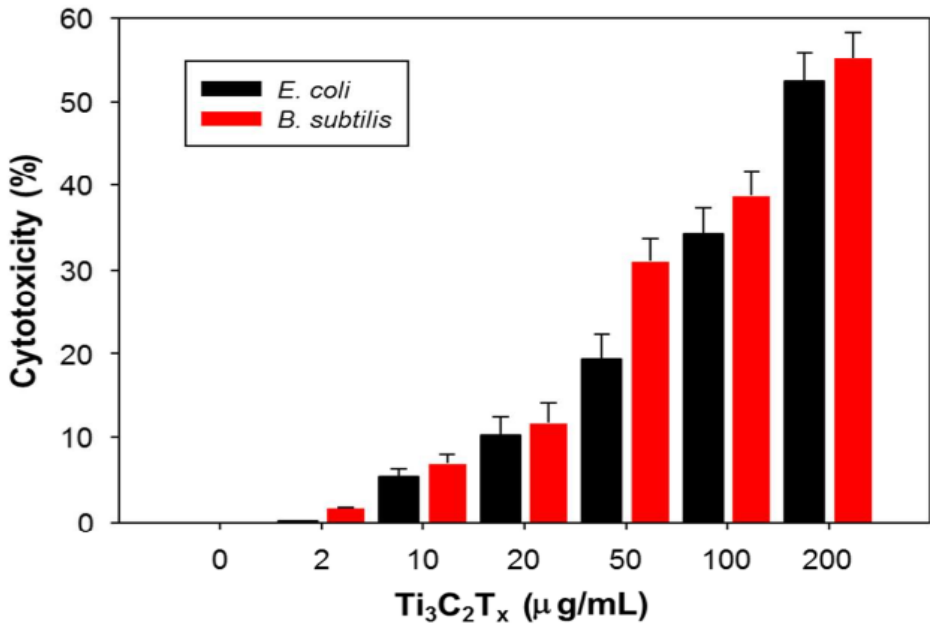

Source: (Rasool *et al*., 2016)

Figure 10. Ti_3C_2Tx cytotoxicity measured by LDH release from the bacterial cells exposed to different concentrations of $Ti_3C_2T_x$ for 4 h.

. Both *E. coli* and *B. subtilis* released very little LDH from the bacterial cells when they were treated to 2 and 10 µg/L of $Ti_3C_2T_x$. However, when bacterial cells were exposed to a 200 µg/L solution of Ti3C2Tx, cytotoxicity of 53.41% and 55.24% for E. coli and B. subtilis, respectively, LDH release rose dramatically. This suggests that both the cell's outside and inside were harmed, which raises the possibility that membrane rupture functions as a significant cell inhibitory mechanism.

3.4 Proposed Antibacterial Mode of Action of MXene nanosheets

Based on the information provided here, we hypothesize that MXene nanosheets with sharp edges enter the bacterial cytoplasm via rupturing the bacterial cell wall, releasing bacterial DNA and ultimately causing bacterial dispersion.

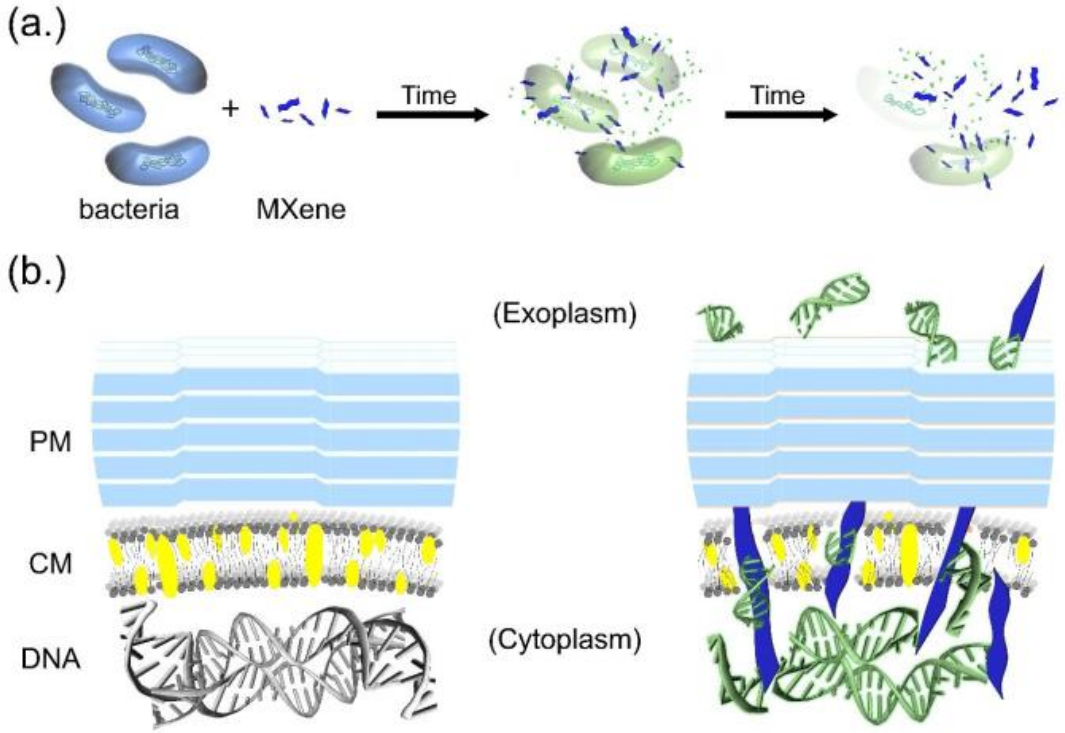

Source: (Shamsabadi *et al*., 2018)

Figure 11. Schematic representation of proposed antibacterial MoA of MXene nanosheets. (a) Interactions of the nanosheets with bacteria cells result in the release of bacteria DNA and eventually bacteria dispersion. (b) MXene sharp nanosheets get into the bacteria cytoplasmic region by cutting the bacteria cell wall. PM and CM stand for peptidoglycan mesh and cytoplasmic membrane, respectively.

The MXene nanosheets' antibacterial activity is size- and exposure- and time-dependent. Indeed, with longer exposure durations, the smaller MXene flake sizes did more harm to the cells. The MXene flakes' sharp (i.e., 1-nm thick) edge will likely pierce the bacterial membranes and reach the cytoplasmic DNA given the typical thickness of bacteria cell walls (i.e., 20–50 nm). Also, by lowering the lateral size of MXene flakes, the number of sharp edges rises and MXene flakes

become more efficient at slicing bacterial membranes. The release of DNA from bacterial cytoplasm happens mostly within the first three hours of the nanosheet treatment. Changes in the morphology and membrane integrity of E. coli and B. subtilis cells as a result of the interaction with Ti3C2Tx were further assessed by SEM and TEM to further understand the antibacterial impact of Ti3C2Tx MXene. Bacterial cells for both E. coli and B. subtilis cultivated without Ti3C2Tx were alive, with no apparent membrane damage or cell death, as shown by SEM images in Figure 12a. The bacteria is shielded by an intact cytoplasmic membrane, as seen by the increased magnification in the lower panels.

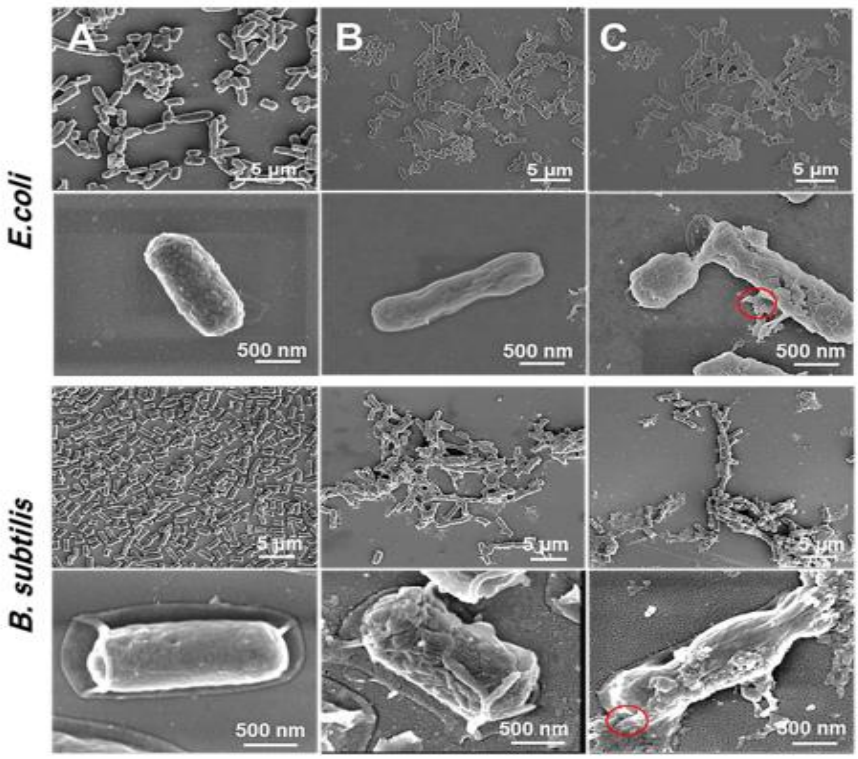

Source: (Rasool *et al.*, 2016)

Figure 12. SEM images of the E. coli (top panel) and B. subtilis (bottom panel) treated with 0 µg/mL – control (A), 50 µg/mL (B), and 100 µg/mL of Ti_3C_2Tx, at low and high magnification, respectively. Control bacterial cells were viable with no observed membrane damage or cell death and the higher magnification shows that the bacterium is protected by intact cytoplasmic membrane (Figure 12A). At 50 and 100 µg/mL of Ti_3C_2Tx, both bacteria suffered from prevalent cell lysis indicated by a severe membrane disruption and cytoplasm leakage (see the red circles at high magnification in Figure 12C).

In contrast, the majority of bacterial cells had widespread membrane damage and cytoplasm leaking in the presence of 50 µg/mL of Ti_3C_2Tx, which is evident at high magnifications (Figure 12B). Several bacterial cells had distorted shapes but still had their membranes intact. Both bacteria experienced widespread cell lysis, as seen by a significant membrane breakdown and cytoplasm leaking, at 100 µg/mL of Ti3C2Tx (see the red circles at high magnification in Figure 12C). Furthermore, the damage to the cell wall and membrane as well as the alteration of the internal structure of the cells were observed using TEM images (Figure 13).

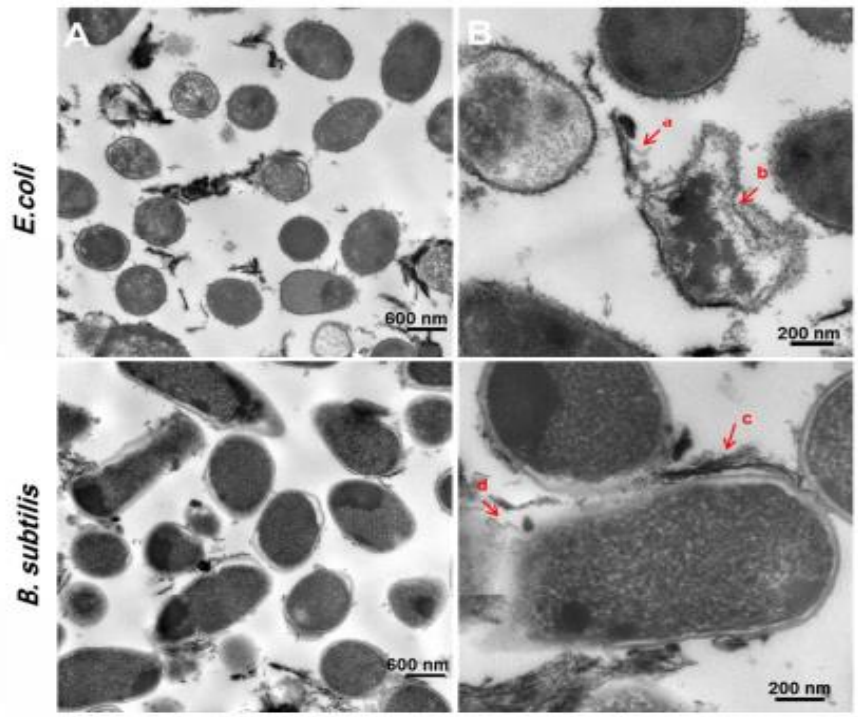

Source: (Rasool *et al.*, 2016)

Figure 13. TEM images of E. coli (A, B) and B. subtilis (C, D) treated with 200 µg/mL of Ti_3C_2Tx for 4 h at low (A, C) and high magnifications (B, D). The cell wall stripped down after exposure to Ti_3C_2Tx nanosheets (arrows b, d), Ti_3C_2Tx nanosheets tightly adsorbed around the cells and entered into the cells (arrows a, c). The intracellular densities of both cells decreased and Ti_3C_2Tx attached to the cellular membrane of both bacteria (arrows b,d).

When E. coli and B. subtilis were exposed to Ti3C2Tx at a concentration of 200 g/mL, TEM examination revealed a reduction in the number of bacterial cells compared to the control group. Ti3C2Tx nanosheets were strongly adhered around the cells in Figure 13, and they even made their

way inside the cells (Figure 13, arrows a, c). Both E. coli and B. subtilis' intracellular densities dropped at the same time, showing that they both lost some intracellular material.

3.5 Prospects of MXenes

It is well known that MXene-based NMs possess a number of amazing properties, including a large precise surface area, exceptionally low cytotoxicity, abundant surface functional groups, and distinct electrical, mechanical, and physicochemical impacts. Calculations have demonstrated that Hf2CO2 MXene is a promising semiconductor with outstanding thermal and electrical characteristics, but it has not yet been produced experimentally. MXenes are promising options for biomedical applications due to their excellent functional characteristics and ease of integration with any systems. MXene-based sensing techniques have been regarded as extremely sophisticated detection methods in a variety of fields, including medicine, the environment, and public health. The very reliable findings provided by the developed MXene sensors/biosensors over a long period of time and their long-term stability make it potentially very advantageous to use these sensors for a variety of diagnostic applications. Nevertheless, because of the lack of information on other transition metal MXene-based detection systems, titanium carbide is the only MXene in the field of sensing that has been extensively studied. The development of appropriate cutting-edge detection methodologies utilizing methods like fluorescence, luminescence, colorimetry, and of course electrochemical for highly selective detection of various biomarkers for early disease identification and point-of-care diagnostic applications will be made possible by advancements in the design of MXene biosensors. Moreover, MXenes have a special promise for tissue engineering, theragnostic, and drug delivery. Based on their permeance and removal capabilities for inorganic and organic solutions, MXene-based membranes have, overall, demonstrated exceptional performance when compared to pristine membranes. MXenes have produced really encouraging outcomes in the adsorptive remediation of polar and ionic contaminants, such as gaseous pollutants, radionuclides, organic dyes, and heavy metal ions. So, the applications of MXenes are diverse. However, the antimicrobial properties of Mxenes are yet to be applied in the real field. Exploring their bactericidal properties, Mxenes can easily be considered as a potent candidate for future biocides.

CHAPTER IV
CONCLUSION

Due to the distinct physiochemical characteristics and ultrathin lamellar structure, two-dimensional (2D) MXenes have showed exceptional antibacterial capabilities. New antimicrobial materials are necessary in order to preserve agricultural production, stop pests from becoming resistant, and provide safe, effective techniques for controlling sickness. According to this review, there is potential in employing MXene nanoparticles as effective biocides in different fields. This review paper demonstrated that the nanosheets' antibacterial activity depends on both their size and their exposure period. The research is still ongoing to fully understand the mode of action of this nanomaterial. Further research should be done to fully explore this materials' tremendous opportunities.

REFERENCES

Akhavan, O., & Ghaderi, E. (2010). Toxicity of graphene and graphene oxide nanowalls against bacteria. *ACS Nano*, *4*(10), 5731–5736. https://doi.org/10.1021/NN101390X/ASSET/IMAGES/MEDIUM/NN-2010-01390X_0006.GIF

Alhabeb, M., Maleski, K., Anasori, B., Lelyukh, P., Clark, L., Sin, S., & Gogotsi, Y. (2017). Guidelines for Synthesis and Processing of Two-Dimensional Titanium Carbide (Ti3C2Tx MXene). *Chemistry of Materials*, *29*(18), 7633–7644. https://doi.org/10.1021/acs.chemmater.7b02847

Anasori, B., Xie, Y., Beidaghi, M., Lu, J., Hosler, B. C., Hultman, L., Kent, P. R. C., Gogotsi, Y., & Barsoum, M. W. (2015). Two-Dimensional, Ordered, Double Transition Metals Carbides (MXenes). *ACS Nano*, *9*(10), 9507–9516. https://doi.org/10.1021/ACSNANO.5B03591/ASSET/IMAGES/NN-2015-03591M_M002.GIF

Shamsabadi, A., Sharifian, M., Anasori, B., & Soroush, M. (2018). Antimicrobial Mode-of-Action of Colloidal Ti3C2Tx MXene Nanosheets. *ACS Sustainable Chemistry and Engineering*, *6*(12), 16586–16596. https://doi.org/10.1021/acssuschemeng.8b03823

Barsoum, M. W. (2013). *MAX phases : properties of machinable ternary carbides and nitrides*. 421. https://www.wiley.com/en-us/MAX+Phases%3A+Properties+of+Machinable+Ternary+Carbides+and+Nitrides-p-9783527654604

Chernousova, S., & Epple, M. (2013). Silver as antibacterial agent: ion, nanoparticle, and metal. *Angewandte Chemie (International Ed. in English)*, *52*(6), 1636–1653. https://doi.org/10.1002/ANIE.201205923

Choi, O., & Hu, Z. (2008). Size dependent and reactive oxygen species related nanosilver toxicity to nitrifying bacteria. *Environmental Science and Technology*, *42*(12), 4583–4588. https://doi.org/10.1021/ES703238H/SUPPL_FILE/ES703238H-FILE002.PDF

Fu, F., Li, L., Liu, L., Cai, J., Zhang, Y., Zhou, J., & Zhang, L. (2015). Construction of cellulose

based ZnO nanocomposite films with antibacterial properties through one-step coagulation. *ACS Applied Materials and Interfaces*, *7*(4), 2597–2606. https://doi.org/10.1021/AM507639B/ASSET/IMAGES/MEDIUM/AM-2014-07639B_0015.GIF

Ganguly, N. K., Arora, N. K., Chandy, S. J., Fairoze, M. N., Gill, J. P. S., Gupta, U., Hossain, S., Joglekar, S., Joshi, P. C., Kakkar, M., Kotwani, A., Rattan, A., Sudarshan, H., Thomas, K., Wattal, C., Easton, M. A., & Laxminarayan, R. (2011). Rationalizing antibiotic use to limit antibiotic resistance in India+. *The Indian Journal of Medical Research*, *134*(3), 281. /pmc/articles/PMC3193708/

Ghidiu, M., Lukatskaya, M. R., Zhao, M. Q., Gogotsi, Y., & Barsoum, M. W. (2014). Conductive two-dimensional titanium carbide 'clay' with high volumetric capacitance. *Nature 2014 516:7529*, *516*(7529), 78–81. https://doi.org/10.1038/nature13970

Ghidiu, M., Naguib, M., Shi, C., Mashtalir, O., Pan, L. M., Zhang, B., Yang, J., Gogotsi, Y., Billinge, S. J. L., & Barsoum, M. W. (2014). Synthesis and characterization of two-dimensional Nb4C3 (MXene). *Chemical Communications*, *50*(67), 9517–9520. https://doi.org/10.1039/C4CC03366C

Gogotsi, Y., & Anasori, B. (2019). The Rise of MXenes. *ACS Nano*, *13*(8), 8491–8494. https://doi.org/10.1021/acsnano.9b06394

Guo, X., Ying, W., Wan, J., Hu, Z., Qian, X., Zhang, H., & He, F. (2001). A comprehensive two-dimensional map of cytosolic proteins of Bacillus subtilis. *Electrophoresis*, *22*(14), 2908–2935. https://doi.org/10.1002/1522-2683(200108)22:14<2908::AID-ELPS2908>3.0.CO;2-M

Halim, J., Lukatskaya, M. R., Cook, K. M., Lu, J., Smith, C. R., Näslund, L. Å., May, S. J., Hultman, L., Gogotsi, Y., Eklund, P., & Barsoum, M. W. (2014). Transparent conductive two-dimensional titanium carbide epitaxial thin films. *Chemistry of Materials*, *26*(7), 2374–2381. https://doi.org/10.1021/CM500641A/SUPPL_FILE/CM500641A_SI_001.PDF

Hu, W., Peng, C., Luo, W., Lv, M., Li, X., Li, D., Huang, Q., & Fan, C. (2010). Graphene-based antibacterial paper. *ACS Nano*, *4*(7), 4317–4323.

https://doi.org/10.1021/NN101097V/SUPPL_FILE/NN101097V_SI_001.PDF

Kim, I. Y., Park, S., Kim, H., Park, S., Ruoff, R. S., & Hwang, S. J. (2014). Strongly-coupled freestanding hybrid films of graphene and layered titanate nanosheets: An effective way to tailor the physicochemical and antibacterial properties of graphene film. *Advanced Functional Materials*, *24*(16), 2288–2294. https://doi.org/10.1002/ADFM.201303040

Klein, E. Y., Van Boeckel, T. P., Martinez, E. M., Pant, S., Gandra, S., Levin, S. A., Goossens, H., & Laxminarayan, R. (2018). Global increase and geographic convergence in antibiotic consumption between 2000 and 2015. *Proceedings of the National Academy of Sciences of the United States of America*, *115*(15), E3463–E3470. https://doi.org/10.1073/PNAS.1717295115

Lakshmi Prasanna, V., & Vijayaraghavan, R. (2015). Insight into the Mechanism of Antibacterial Activity of ZnO: Surface Defects Mediated Reactive Oxygen Species even in the Dark. *Langmuir*, *31*(33), 9155–9162. https://doi.org/10.1021/ACS.LANGMUIR.5B02266/SUPPL_FILE/LA5B02266_SI_001.PDF

Lei, J. C., Zhang, X., & Zhou, Z. (2015). Recent advances in MXene: Preparation, properties, and applications. *Frontiers of Physics*, *10*(3), 276–286. https://doi.org/10.1007/s11467-015-0493-x

Lemire, J. A., Harrison, J. J., & Turner, R. J. (2013). Antimicrobial activity of metals: mechanisms, molecular targets and applications. *Nature Reviews Microbiology 2013 11:6*, *11*(6), 371–384. https://doi.org/10.1038/nrmicro3028

Li, J., Wang, G., Zhu, H., Zhang, M., Zheng, X., Di, Z., Liu, X., & Wang, X. (2014). Antibacterial activity of large-area monolayer graphene film manipulated by charge transfer. *Scientific Reports 2014 4:1*, *4*(1), 1–8. https://doi.org/10.1038/srep04359

Li, Q., Mahendra, S., Lyon, D. Y., Brunet, L., Liga, M. V., Li, D., & Alvarez, P. J. J. (2008). Antimicrobial nanomaterials for water disinfection and microbial control: potential applications and implications. *Water Research*, *42*(18), 4591–4602. https://doi.org/10.1016/J.WATRES.2008.08.015

Li, Y., Zhang, W., Niu, J., & Chen, Y. (2012). Mechanism of photogenerated reactive oxygen species and correlation with the antibacterial properties of engineered metal-oxide nanoparticles. *ACS Nano*, *6*(6), 5164–5173. https://doi.org/10.1021/NN300934K/SUPPL_FILE/NN300934K_SI_001.PDF

Liu, S., Zeng, T. H., Hofmann, M., Burcombe, E., Wei, J., Jiang, R., Kong, J., & Chen, Y. (2011). Antibacterial activity of graphite, graphite oxide, graphene oxide, and reduced graphene oxide: Membrane and oxidative stress. *ACS Nano*, *5*(9), 6971–6980. https://doi.org/10.1021/NN202451X/SUPPL_FILE/NN202451X_SI_001.PDF

Mashtalir, O., Cook, K. M., Mochalin, V. N., Crowe, M., Barsoum, M. W., & Gogotsi, Y. (2014). Dye adsorption and decomposition on two-dimensional titanium carbide in aqueous media. *Journal of Materials Chemistry A*, *2*(35), 14334–14338. https://doi.org/10.1039/C4TA02638A

Mashtalir, O., Lukatskaya, M. R., Zhao, M. Q., Barsoum, M. W., & Gogotsi, Y. (2015). Amine-Assisted Delamination of Nb2C MXene for Li-Ion Energy Storage Devices. *Advanced Materials (Deerfield Beach, Fla.)*, *27*(23), 3501–3506. https://doi.org/10.1002/ADMA.201500604

Mashtalir, O., Naguib, M., Mochalin, V. N., Dall'Agnese, Y., Heon, M., Barsoum, M. W., & Gogotsi, Y. (2013). Intercalation and delamination of layered carbides and carbonitrides. *Nature Communications*, *4*. https://doi.org/10.1038/NCOMMS2664

Naguib, M., & Gogotsi, Y. (2015). Synthesis of two-dimensional materials by selective extraction. *Accounts of Chemical Research*, *48*(1), 128–135. https://doi.org/10.1021/AR500346B

Naguib, M., Halim, J., Lu, J., Cook, K. M., Hultman, L., Gogotsi, Y., & Barsoum, M. W. (2013). New two-dimensional niobium and vanadium carbides as promising materials for li-ion batteries. *Journal of the American Chemical Society*, *135*(43), 15966–15969. https://doi.org/10.1021/JA405735D/SUPPL_FILE/JA405735D_SI_001.PDF

Naguib, M., Kurtoglu, M., Presser, V., Lu, J., Niu, J., Heon, M., Hultman, L., Gogotsi, Y., & Barsoum, M. W. (2011). Two-dimensional nanocrystals produced by exfoliation of Ti 3AlC

2. *Advanced Materials*, *23*(37), 4248–4253. https://doi.org/10.1002/adma.201102306

Naguib, M., Mashtalir, O., Carle, J., Presser, V., Lu, J., Hultman, L., Gogotsi, Y., & Barsoum, M. W. (2012). Two-dimensional transition metal carbides. *ACS Nano*, *6*(2), 1322–1331. https://doi.org/10.1021/NN204153H

Naguib, M., Unocic, R. R., Armstrong, B. L., & Nanda, J. (2015). Large-scale delamination of multi-layers transition metal carbides and carbonitrides "MXenes." *Dalton Transactions*, *44*(20), 9353–9358. https://doi.org/10.1039/C5DT01247C

Narayan, R. J., Berry, C. J., & Brigmon, R. L. (2005). Structural and biological properties of carbon nanotube composite films. *Materials Science and Engineering B*, *123*, 123–129. https://doi.org/10.1016/j.mseb.2005.07.007

Pandey, R. P., Rasheed, P. A., Gomez, T., Rasool, K., Ponraj, J., Prenger, K., Naguib, M., & Mahmoud, K. A. (2020). Effect of Sheet Size and Atomic Structure on the Antibacterial Activity of Nb-MXene Nanosheets. *ACS Applied Nano Materials*, *3*(11), 11372–11382. https://doi.org/10.1021/acsanm.0c02463

Pimentel, D., & Burgess, M. (2012). Small amounts of pesticides reaching target insects. *Environment, Development and Sustainability*, *14*(1), 1–2. https://doi.org/10.1007/S10668-011-9325-5

Pulskamp, K., Diabaté, S., & Krug, H. F. (2007). Carbon nanotubes show no sign of acute toxicity but induce intracellular reactive oxygen species in dependence on contaminants. *Toxicology Letters*, *168*(1), 58–74. https://doi.org/10.1016/J.TOXLET.2006.11.001

Ramanan Laxminarayan, Thomas Van Boeckel, A. T. (2015). The Economic Costs of Withdrawing Antimicrobial Growth Promoters from the Livestock Sector. *Journal of Forestry*, *32*(6), 209–213. https://doi.org/10.1787/5js64kst5wvl-en

Rasool, K., Helal, M., Ali, A., Ren, C. E., Gogotsi, Y., & Mahmoud, K. A. (2016). Antibacterial Activity of Ti3C2Tx MXene. *ACS Nano*, *10*(3), 3674–3684. https://doi.org/10.1021/acsnano.6b00181

Salas, E. C., Sun, Z., Lüttge, A., & Tour, J. M. (2010). Reduction of graphene oxide via bacterial

respiration. *ACS Nano*, *4*(8), 4852–4856. https://doi.org/10.1021/NN101081T

Tao, Q., Dahlqvist, M., Lu, J., Kota, S., Meshkian, R., Halim, J., Palisaitis, J., Hultman, L., Barsoum, M. W., Persson, P. O. Å., & Rosen, J. (2017). Two-dimensional Mo1.33C MXene with divacancy ordering prepared from parent 3D laminate with in-plane chemical ordering. *Nature Communications 2017 8:1*, *8*(1), 1–7. https://doi.org/10.1038/ncomms14949

Tu, Y., Lv, M., Xiu, P., Huynh, T., Zhang, M., Castelli, M., Liu, Z., Huang, Q., Fan, C., Fang, H., & Zhou, R. (2013). Destructive extraction of phospholipids from Escherichia coli membranes by graphene nanosheets. *Nature Nanotechnology*, *8*(8), 594–601. https://doi.org/10.1038/NNANO.2013.125

Van Boeckel, T. P., Brower, C., Gilbert, M., Grenfell, B. T., Levin, S. A., Robinson, T. P., Teillant, A., & Laxminarayan, R. (2015). Global trends in antimicrobial use in food animals. *Proceedings of the National Academy of Sciences of the United States of America*, *112*(18), 5649–5654. https://doi.org/10.1073/PNAS.1503141112/SUPPL_FILE/PNAS.201503141SI.PDF

Wang, D., Saleh, N. B., Byro, A., Zepp, R., Sahle-Demessie, E., Luxton, T. P., Ho, K. T., Burgess, R. M., Flury, M., White, J. C., & Su, C. (2022). Nano-enabled pesticides for sustainable agriculture and global food security. *Nature Nanotechnology 2022 17:4*, *17*(4), 347–360. https://doi.org/10.1038/s41565-022-01082-8

Wang, Y. W., Cao, A., Jiang, Y., Zhang, X., Liu, J. H., Liu, Y., & Wang, H. (2014). Superior antibacterial activity of zinc oxide/graphene oxide composites originating from high zinc concentration localized around bacteria. *ACS Applied Materials and Interfaces*, *6*(4), 2791–2798. https://doi.org/10.1021/AM4053317/SUPPL_FILE/AM4053317_SI_001.PDF

Wu, L., Zeng, L., & Jiang, X. (2015). Revealing the nature of interaction between graphene oxide and lipid membrane by surface-enhanced infrared absorption spectroscopy. *Journal of the American Chemical Society*, *137*(32), 10052–10055. https://doi.org/10.1021/JACS.5B03803/SUPPL_FILE/JA5B03803_SI_001.PDF

Zhang, W., Li, Y., Niu, J., & Chen, Y. (2013). Photogeneration of reactive oxygen species on uncoated silver, gold, nickel, and silicon nanoparticles and their antibacterial effects.

Langmuir : The ACS Journal of Surfaces and Colloids, *29*(15), 4647–4651. https://doi.org/10.1021/LA400500T